8-2010

Cylinder light concentrator and absorber: theoretical description

Alexander V. Kildishev
Birck Nanotechnology Center, School of ECE, kildishev@purdue.edu

Ludmila J. Prokopeva
Russian Acad Sci

Evgenii Narimanov
Purdue University, evgenii@purdue.edu

Kildishev, Alexander V.; Prokopeva, Ludmila J.; and Narimanov, Evgenii, "Cylinder light concentrator and absorber: theoretical description" (2010). *Birck and NCN Publications.* Paper 691.
http://dx.doi.org/10.1364/OE.18.016646

Cylinder light concentrator and absorber: theoretical description

Alexander V. Kildishev,[1,*] Ludmila J. Prokopeva,[2] and Evgenii E. Narimanov[1]

[1] *Birck Nanotechnology Center, School of Electrical Engineering, Purdue University, West Lafayette IN 47903 USA*
[2] *Institute of Computational Technologies, Russian Academy of Sciences, Novosibirsk, Russia*
**kildishev@purdue.edu*

Abstract: We present a detailed theoretical description of a broadband omnidirectional light concentrator and absorber with cylinder geometry. The proposed optical "trap" captures nearly all the incident light within its geometric cross-section, leading to a broad range of possible applications – from solar energy harvesting to thermal light emitters and optoelectronic components. We have demonstrated that an approximate lamellar black-hole with a moderate number of homogeneous layers, while giving the desired ray-optical performance, can provide absorption efficiencies comparable to those of ideal devices with a smooth gradient in index.

OCIS codes: (260.0260) Physical Optics; (070.7345) Wave propagation

References and links

1. V. M. Shalaev, W. S. Cai, U. K. Chettiar, H. K. Yuan, A. K. Sarychev, V. P. Drachev, and A. V. Kildishev, "Negative index of refraction in optical metamaterials," Opt. Lett. **30**(24), 3356–3358 (2005).
2. J. B. Pendry, "Negative refraction makes a perfect lens," Phys. Rev. Lett. **85**(18), 3966–3969 (2000).
3. Z. Jacob, L. V. Alekseyev, and E. Narimanov, "Optical Hyperlens: Far-field imaging beyond the diffraction limit," Opt. Express **14**(18), 8247–8256 (2006).
4. A. Salandrino and N. Engheta, "Far-Field Subdiffraction Optical Microscopy Using Metamaterial Crystals: Theory and Simulations," Phys. Rev. B **74**(7), 075103 (2006).
5. N. M. Litchinitser, and V. M. Shalaev, "Metamaterials: transforming theory into reality," J. Opt. Soc. Am. B **26**(12), B161–B169 (2009).
6. N. I. Landy, S. Sajuyigbe, J. J. Mock, D. R. Smith, and W. J. Padilla, "Perfect metamaterial absorber," Phys. Rev. Lett. **100**(20), 207402 (2008).
7. T. V. Teperik, F. J. García de Abajo, A. G. Borisov, M. Abdelsalam, P. N. Bartlett, Y. Sugawara, and J. J. Baumberg, "Omnidirectional absorption in nanostructured metal surfaces," Nat. Photonics **2**(5), 299–301 (2008).
8. E. E. Narimanov, and A. V. Kildishev, "Optical black hole: broadband omnidirectional light absorber," Appl. Phys. Lett. **95**(4), 041106 (2009).
9. L. D. Landau, and E. M. Lifshitz, Mechanics, Pergamon Press, Oxford, (1976).
10. R. K. Luneburg, Mathematical Theory of Optics, University of California Press, Berkeley, 1964, p. 12.
11. E. J. Post, Formal Structure of Electromagnetics: General Covariance and Electromagnetics, 1962, p. 152.
12. S. Gradshteyn, and I. M. Ryzhik, Tables of integrals, series and products, Academic Press, New York, CD-ROM Edition, 1994, Eq. (8).511.4.
13. M. Born, and E. Wolf, Principles of Optics, Electromagnetic Theory of Propagation, Interference and Diffraction of Light, 7th ed. (Cambridge University Press, New York, 1999).
14. G. P. Agrawal, and D. N. Pattanayak, "Gaussian beam propagation beyond the paraxial approximation," J. Opt. Soc. Am. **69**(4), 575 (1979).
15. M. Abramowitz, and I. A. Stegun, eds., Handbook of Mathematical Functions with Formulas, Graphs, and Mathematical Tables, New York, Dover, (1972).
16. V. Kildishev, U. K. Chettiar, Z. Jacob, V. M. Shalaev, and E. E. Narimanov, "Materializing a binary hyperlens design," Appl. Phys. Lett. **94**(7), 071102 (2009).
17. S. D. Conte, and C. W. Boor, "Elementary Numerical Analysis: An Algorithmic Approach, 3rd edition," 1980.
18. H. Hulst, Light scattering by small particles, Dover, 1981, p. 309.

1. Introduction

Recent advances in the development of optical metamaterials, artificial structures with the desired local electromagnetic response determined by artificial subwavelength patterning of the media, have opened a wide range of new concepts and applications, from super-resolution

#126127 - $15.00 USD Received 30 Mar 2010; revised 19 Jun 2010; accepted 29 Jun 2010; published 23 Jul 2010

imaging to optoelectronics and photovoltaics [1–8]. In particular, the recently proposed [8] "optical black hole", an omnidirectional light concentrator and absorber, could significantly enhance the performance of solar energy harvesting systems and lead to novel nonlinear-optical devices. In this work, we present a detailed theoretical description of this device, and develop appropriate numerical methods, which – in addition to the accurate analysis of the optical black hole, - could be applied to a broad range of metamaterial-based optical systems with centrally symmetric gradient index. We note that in the context of this paper, the term "black hole" simply refers to the highly efficient "capture" of the light incident on the device, and does not imply any profound analogy to General Relativity.

The remaining part of the paper is organized as follows. In Section 2, we introduce the initial assumptions, state the geometry of the cylindrical optical system with an axially symmetric graded index, and show basic examples of ray-tracing inside such devices, including the fundamental optical black-hole [8]. Section 3 deals with the ray optical description of the system followed by its full-wave description in Section 4. The analytical and numerical apparatus for approximating the ideal fundamental black-hole with concentric lamellar systems of uniform isotropic layers is then discussed in Section 5. Section 5 also covers derivations of the scattering and absorption cross-sections, which are then compared with their semiclassical approximations in Section 6. Finally, we summarize our work in Section 7.

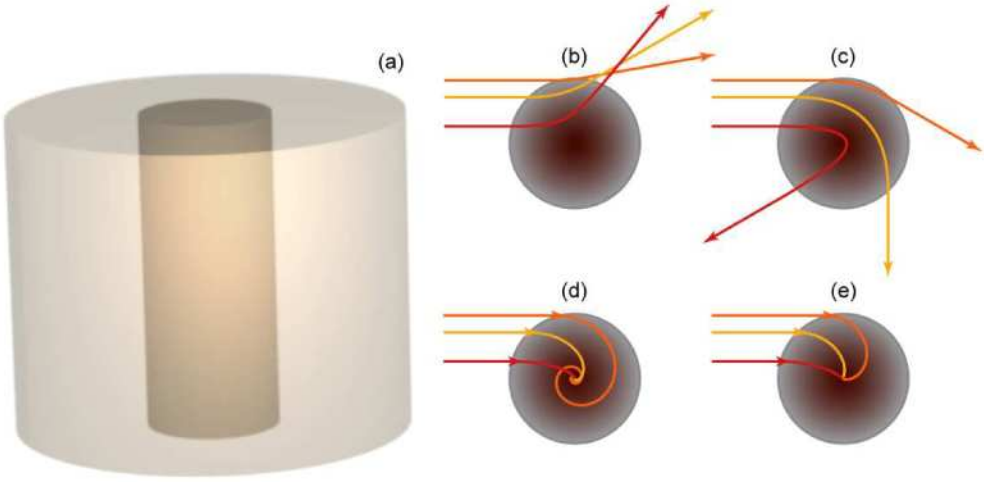

Fig. 1. (a) the schematics of the system; panels (b), (c), (d), and (e) show light ray trajectories for p equal to –1, 1, 2, and 3 respectively, where core radius r_c much smaller than shell radius r_s ($r_c = r_s$).

2. The system

In its original proposal [8], the optical "black hole" (see Fig. 1(a)) consists of the "payload" core with the radius r_c, supporting the desired functionality (such as e.g. a solar cell for concentrated photovoltaics applications), surrounded by the concentrating shell of radius r_s with an axially symmetric dielectric function, $\varepsilon(r)$, changing in the radial direction as

$$\varepsilon(r) \equiv \varepsilon_s \Delta\varepsilon(r) \tag{1}$$

where

#126127 - $15.00 USD Received 30 Mar 2010; revised 19 Jun 2010; accepted 29 Jun 2010; published 23 Jul 2010

$$\Delta\varepsilon(r)=\begin{cases}1, & r>r_s\\ \left(r_s/r\right)^p, & r_c<r\le r_s\\ \left(\varepsilon_c+\imath\gamma\right)/\varepsilon_s, & r\le r_c\end{cases} \tag{2}$$

and $p>0$ is a constant. In order to match the real parts of relative permittivity at the interface $r=r_c$ the radius of the core is defined by the ratio of the permittivity of the surrounding medium (ε_s) to that of the core (ε_c),

$$r_c=r_s\left(\varepsilon_s/\varepsilon_c\right)^{1/p}. \tag{3}$$

Note that we assume that the metamaterial forming the shell, is essentially non-magnetic, so that the refractive index is $n=\sqrt{\varepsilon}$.

3. Ray-optical description

In the semi-classical limit, the radial variation of the refractive index of the shell (where $n=\sqrt{\varepsilon}$) corresponds to the effective potential

$$V_{eff}\left(r\right)=\tfrac{1}{2}\left(\omega/c\right)^2\left[\varepsilon_s-\varepsilon\left(r\right)\right], \tag{4}$$

which for the dielectric permittivity defined by (2) with $p\ge 2$ traps all the incident light trajectories – see Figs. 1(b)-1(e). For these ray trajectories, a straightforward integration of the Hamiltonian equations with the effective potential defined by (4) yields in the polar coordinates

$$\phi(r)=\phi_0+\int_{\frac{m}{r_s}}^{\frac{m}{r}}\frac{d\xi}{\sqrt{C_0\varepsilon\left(m/\xi\right)-\xi^2}}, \tag{5}$$

where m is the (conserved) angular momentum, $C_0=\left(m/y_0\right)^2/\varepsilon_s$ (with y_0 being $r_s\sin\phi_0$), and the constants r_s and ϕ_0 are set by the initial conditions of the given trajectory. In particular, for the permittivity defined in the shell (2), Eq. (5) after integration gives

$$r\left(\phi\right)=r_s\times\begin{cases}\left|\csc\phi_0\cos\left[\frac{p-2}{2}\left(\phi-\phi_p\right)\right]\right|^{\frac{2}{p-2}}, & p\ne 2\\ \exp\left[\cot\phi_0\left(\phi_0-\phi\right)\right], & p=2\end{cases}, \tag{6}$$

where ϕ_p is yet another constant defined by $\phi_p=\phi_0\left(1-\frac{2}{p-2}\right)+\frac{\pi}{p-2}$.

Case $p=1$ corresponds to the gravitational potential (or electrostatic potential) and emulates the motion of a non-accelerated particle in central gravitational field; so that the parabolic trajectories (Fig. 1c) are expected. Case $p=2$ gives the potential of fatal attraction [9]. In fact for all $p\ge 2$ (6) corresponds to the ray trajectories "falling" into the core of the "black hole" – see Fig. 1(b). Figures 1(b)-1(e) show the traces of light rays for p equal to –1, 1, 2, and 3 respectively; the trivial case of the beam propagating in free-space ($p=0$) is omitted.

This concept can be realized in both the spherical and cylindrical geometries, with the latter suitable for optoelectronic devices where the light propagation is generally realized in a

#126127 - $15.00 USD Received 30 Mar 2010; revised 19 Jun 2010; accepted 29 Jun 2010; published 23 Jul 2010

waveguide geometry. In the present paper we will focus on this cylindrical realization of the optical black hole, leaving its spherical counterpart to a forthcoming work.

4. The wave optical description

In the present section of the paper, we develop the wave-optical description of the "black hole" light concentrator. We define a given monochromatic electromagnetic vector field by the vectors of electric field $\mathbf{E}\exp(-\imath\omega t)$ and magnetic field $\mathbf{H}\exp(-\imath\omega t)$, and by its angular frequency ω. We start with the monochromatic Maxwell's equations $\nabla\times\mathbf{E}=\imath\omega\mathbf{B}$, $\nabla\times\mathbf{H}=-\imath\omega\mathbf{D}$ arriving first at [10]:

$$k_0^2\varepsilon\mu\mathbf{H}=\nabla\times\nabla\times\mathbf{H}-\nabla\ln\varepsilon\times\nabla\times\mathbf{H}, \tag{7}$$

$$k_0^2\varepsilon\mu\mathbf{E}=\nabla\times\nabla\times\mathbf{E}-\nabla\ln\mu\times\nabla\times\mathbf{E}. \tag{8}$$

Getting $\nabla\cdot\mathbf{H}=-\nabla\ln\mu\cdot\mathbf{H}$, $\nabla\cdot\mathbf{E}=-\nabla\ln\varepsilon\cdot\mathbf{E}$ from $\nabla\cdot\mathbf{B}=\nabla\cdot\mathbf{D}=0$, we then rewrite (7)-(8) as

$$k^2\mathbf{H}+\nabla^2\mathbf{H}=-\nabla\left(\nabla\ln\mu\cdot\mathbf{H}\right)-\nabla\ln\varepsilon\times\nabla\times\mathbf{H}, \tag{9}$$

$$k^2\mathbf{E}+\nabla^2\mathbf{E}=-\nabla\left(\nabla\ln\varepsilon\cdot\mathbf{E}\right)-\nabla\ln\mu\times\nabla\times\mathbf{E}. \tag{10}$$

here $k^2=\varepsilon k_0^2$, $k_0^2=\omega^2/c^2$, and $c^2=1/(\varepsilon_0\mu_0)$, where $\varepsilon=\varepsilon(x,y)$ is a smooth spatially-dependent dielectric function, the free-space parameters k_0, c, ε_0, and μ_0 respectively denote the wavenumber, the velocity of light, the permittivity, and the permeability.

Here we assume only transverse electric (TE, $\mathbf{E}=\hat{\mathbf{z}}e(x,y)$) and transverse magnetic (TM, $\mathbf{H}=\hat{\mathbf{z}}h(x,y)$) waves within a nonmagnetic medium ($\mu=1$), so we reduce the above vector equations and use in-plane scalars e and h, which are further on collectively denoted as f.

4.1 Scalar wave equations and separation of variables

Hence, both TE and TM wave Eqs. (9) and (10) reduce to a common scalar wave equation

$$\nabla^2 f+k^2 f+Lf=0. \tag{11}$$

For any TM-wave ($f=h$) the operator L is given by $L=-\nabla\ln\varepsilon\cdot\nabla$ and does not vanish for spatially dispersive ε, while it vanishes for any TE-wave ($f=e$).

The cylindrical symmetry of the device allows a straightforward separation of radial and angular variables in the cylindrical coordinates, (r, ϕ, z), linked to the Cartesian coordinates (x, y, z) through $x=r\cos\phi$, $y=r\sin\phi$. Exploiting the cylindrical symmetry of the dielectric function, $\varepsilon=\varepsilon(r)$, and decomposing the solution of (11) into the cylindrical waves, $f=\sum_{m=-\infty}^{+\infty}f_m(r)\exp\imath m\phi$, we arrive at equation for scalar modes f_m

$$r^2 f_m''+\left[r+q(r)\right]f_m'+\left[k^2r^2-m^2\right]f_m=0, \tag{12}$$

where the prime denotes the radial derivative, and $q(r)=0$ or $q(r)=-r^2\ln'\varepsilon$ for TE or TM modes respectively.

#126127 - $15.00 USD Received 30 Mar 2010; revised 19 Jun 2010; accepted 29 Jun 2010; published 23 Jul 2010

4.2 TE and TM solutions for $\varepsilon(r) = \text{const}$

The solvable cases that we are using here include the trivial instance of $\varepsilon(r) = \text{const}$ for both TE and TM modes. In this case, (12) reduces to the Bessel equation for $\overline{r} = kr$, and the general solution is a linear combination of two linearly independent Bessel functions [11].

In most of the cases it is more convenient to use the following combination

$$f_m(r) = a_m J_m(\overline{r}) + b_m H_m^+(\overline{r}), \tag{13}$$

since it represents the unique decomposition (usually found in scattering problems) into the incident and scattered field if the domain is infinite. On the other hand if the solution is written in the domain, which contains the origin, then the additional boundary condition should be provided to avoid singularity ($b_m = 0$).

For simulations we use the normalized variant of (13), which improves the condition number of the linear system matrix (Section 5.1):

$$f_m(r) = \tau_m J_m(\overline{r}) / J_m(\overline{r}_s) + \rho_m H_m^+(\overline{r}) / H_m^+(\overline{r}_s). \tag{14}$$

However in some applications, including the calculation of cross sections, a better option is an equivalent combination of the Hankel functions $H_m^{\pm}(\overline{r}) = J_m(\overline{r}) \pm \imath Y_m(\overline{r})$

$$f_m(r) = c_m^- H_m^-(\overline{r}) + c_m^+ H_m^+(\overline{r}), \tag{15}$$

which gives expressions that are easier to handle for mathematical analyses (Section 5.3). Back and forth translations between formulas (13) and (15) are performed by $c_m^- = \frac{1}{2} a_m$, $c_m^+ = \frac{1}{2}(a_m + 2b_m)$, and $a_m = 2c_m^-$, $b_m = c_m^+ - c_m^-$.

4.3 TE and TM solutions for the 'quadratic decay' of permittivity, $r^2\varepsilon(r) = \text{const}$

For the cylindrical realization of the black hole, which in its simplest form corresponds to an infinite cylinder with a radial distribution of the dielectric permittivity given by $r^2\varepsilon(r) = \text{const}$ or $k^2 r^2 = \nu^2 = \text{const}$, all optical modes of the system can also be separated into the TE and TM categories. For the TM wave $q(r) = -r^2 \ln' \varepsilon = 2r$, while for TE we always have $q(r) = 0$.

For a TM mode, (12) can be therefore reduced as

$$r^2 f_m'' + 3r f_m' + [\nu^2 - m^2] f_m = 0, \tag{16}$$

and for a TE mode as

$$r^2 f_m'' + r f_m' + [\nu^2 - m^2] f_m = 0. \tag{17}$$

Both (16) and (17) are the Euler differential equations, which are solved by substitution $s = \ln r$. Then, since $r^2 f'' + r f' = \partial_s^2 f$ and $r f' = \partial_s f$ we arrive at the characteristic equation for $f(\exp s)$ with roots $\xi_{1,2}$, where the general solution reads

$$f_m(r) = \begin{cases} a_m r^{\xi_1} + b_m r^{\xi_2}, & \text{if } \xi_1 \neq \xi_2 \\ (a_m + b_m \ln r) r^{\xi_1}, & \text{otherwise} \end{cases} \tag{18}$$

and the characteristic roots $\xi_{1,2}$ in (18) are

#126127 - $15.00 USD Received 30 Mar 2010; revised 19 Jun 2010; accepted 29 Jun 2010; published 23 Jul 2010

$$\xi_{1,2} = \begin{cases} -1 \pm \imath\sqrt{\nu^2 - m^2 - 1}, & (\mathrm{TE}) \\ \pm\imath\sqrt{\nu^2 - m^2}, & (\mathrm{TM}) \end{cases} \tag{19}$$

or equivalently, $\xi_{1,2} = -\alpha \pm \imath\beta_m$, where $\alpha = 1$ for TM, or $\alpha = 0$ for TE, and $\beta_m = \sqrt{\nu^2 - m^2 - \alpha}$ in both cases.

4.4 Boundary conditions and the mode matching

In previous sections the general analytical solutions were written in the domains, where the dielectric function $\varepsilon(r)$ is defined by either the Bessel equation or the Euler equation. At each interface between such domains, the electromagnetic field should satisfy the standard boundary conditions for the continuity of the tangential components of the magnetic and electric fields. Furthermore, the physical requirement for the behavior at the infinity and at the origin, introduce additional constrains to the solution, as described earlier in Section 4.2

In particular for a nonmagnetic, cylindrically symmetric medium without any free charges the condition of continuity of electromagnetic fields at a given interface $r = r_i > 0$ reads

TE:

$$[e]_{r=r_i} = [e']_{r=r_i} = 0, \tag{20}$$

TM:

$$[h]_{r=r_i} = [\varepsilon^{-1}h']_{r=r_i} = 0, \tag{21}$$

where $[f(r)]_{r=r_i} = \lim_{a\to 0} f(r_i + a) - \lim_{a\to 0} f(r_i - a)$. Since we assume that both the inner and outer sub-domains are of constant permittivity, with the general solution given by Eq. (13), which should have a physical solution at $r = 0$, then $b_m = 0$ and

$$f_m(r) = a_m J_m(kr). \tag{22}$$

If the function f describes the scattered field (i.e. does not include the incident wave), it should obey the Sommerfeld radiation condition, $\lim_{r\to\infty}\sqrt{r}(f' - \imath kf) = 0$. The asymptotic behavior of the Hankel functions $H_m^{\pm}(kr) \sim r^{-1/2}e^{\pm\imath kr}$ for $r \to \infty$ forces us to choose only one term in (13); hence, for the scattered field we have

$$f_m(r) = b_m H_m^{+}(kr). \tag{23}$$

4.5 Incident light: the Gaussian beams and plane wave

While the angular momentum formalism introduced above, represents the "natural" choice for a system with rotational symmetry, to complete the description of the scattering problem, we also need to develop the angular momentum expansion of the incident field. Here, we will consider the most common examples of the illumination field: the plane wave and the Gaussian beam.

Starting from the classical generating function for the Bessel functions [12]:

$$\exp(\imath z\cos\varphi) = \sum \imath^m e^{\imath m\varphi} J_m(z), \tag{24}$$

for the incident plane wave we obtain ($a_m = \imath^m$)

#126127 - $15.00 USD Received 30 Mar 2010; revised 19 Jun 2010; accepted 29 Jun 2010; published 23 Jul 2010

$$f(x,y) = e^{\imath kx} = \sum_{m=-\infty}^{+\infty} a_m J_m(kr) e^{\imath m\varphi}. \tag{25}$$

While plane wave illumination represents perhaps the most common setup of a scattering problem, it does not convey the case when the target is illuminated by a focused beam. The latter is generally adequately described by the Gaussian beam [13], which yields an accurate description of the beam focused by linear optical elements. However, one needs to keep in mind that the Gaussian beam in its standard form is *not* an exact solution of Maxwell's equations in the free space, but instead corresponds to the paraxial approximation [13]. To avoid the approximate nature of this approach and resulting inaccuracy, we consider that the field, while following the Gaussian profile at the waist cross section, is in fact the exact solution of the Helmholtz wave equation with the given direction of propagation [14]:

$$\begin{cases} \nabla^2 f + k^2 f = 0 \\ f(0,y) = \exp\left[-(y/w)^2\right] \end{cases} \tag{26}$$

The resulting solution of (26) in each of half-spaces $y \le 0$, $y \ge 0$ can be written as a composition of *y*-plane waves

$$f(x,y) = \int_{-1}^{1} a_q \exp\left[\imath k\left(qy + \sqrt{1-q^2}\,x\right)\right] dq + \int_{|q|>1} a_q \exp\left[\imath kqy - k\sqrt{q^2-1}\,|x|\right] dq, \tag{27}$$

where the amplitudes $a_q = \frac{1}{2\sqrt{\pi}} kw \exp\left[-\frac{1}{4}(kwq)^2\right]$ satisfy the condition $e^{-y^2/w^2} = \int_{-\infty}^{\infty} a_q e^{\imath kyq} dq$. Here, the field is separated into the contributions of the propagating (the first integral in (27)) and the evanescent waves (the second term in (27)). The contribution of evanescent waves, can be estimated as

$$\sigma = \left| \int_{|q|>1} a_q \exp\left[\imath kqy - k\sqrt{q^2-1}\,|x|\right] dq \right| \le \frac{kw}{\sqrt{\pi}} \int_{1}^{+\infty} e^{-\frac{1}{4}k^2w^2q^2} dq = \operatorname{erfc}\left(\tfrac{1}{2}kw\right). \tag{28}$$

As a result of (28), for a Gaussian beam with waist $w \ge 2\lambda$ propagating in media with $\varepsilon \ge 1$ neglecting the evanescent waves integral in (27) gives a reasonable approximation, since the relative error of the field magnitude is less than $\operatorname{erfc}\left(\frac{1}{2}kw\right) \le \operatorname{erfc}(2\pi) \approx 6\times10^{-19}$.

Adding the arbitrary shift of the focus location by straightforward translation, $x \to x - x_0$, $y \to y - y_0$, the final expression of a focused beam in Cartesian coordinates is

$$f(x,y) = \frac{kw}{2\sqrt{\pi}} \int_{-1}^{1} e^{-\frac{1}{4}k^2w^2q^2 + \imath k\left[q(y-y_0) + \sqrt{1-q^2}(x-x_0)\right]} dq, \tag{29}$$

or (29) can be equivalently written in the cylindrical coordinates with $x = r\cos\phi$ and $y = r\sin\phi$ giving

$$f(r,\phi) = \frac{kw}{2\sqrt{\pi}} \int_{-1}^{1} e^{-\frac{1}{4}k^2w^2q^2 - \imath k\left(qy_0 + \sqrt{1-q^2}x_0 - r\cos[\phi - \psi(q)]\right)} dq, \tag{30}$$

where $\psi(q) = \sin^{-1} q$.

#126127 - $15.00 USD Received 30 Mar 2010; revised 19 Jun 2010; accepted 29 Jun 2010; published 23 Jul 2010

Using the generating function (24) for $z = kr$ and $\varphi = \phi - \psi(q)$ we obtain from (30) the final series

$$f(r,\phi) = \sum_{m=-\infty}^{+\infty} a_m J_m(kr) e^{\imath m\phi}, \tag{31}$$

where $a_m = \frac{kw}{2\sqrt{\pi}} \imath^m \int_{-1}^{1} \exp\left[-\frac{1}{4}k^2 w^2 q^2 - \imath k\left(q y_0 + \sqrt{1-q^2}\, x_0 \right) - \imath m \sin^{-1} q \right] dq$.

5. Layered Systems

Practical realizations of concentric cylinder optical and optoelectronic devices often involve a design that includes a number of (homogeneous) layers. In particular, external layers may be incorporated as a protective cover, while an internal layer between the absorber and the shell of the optical concentrator provides additional mechanical support or works as a channel for a liquid absorber. In this Section, we develop the theoretical description of light scattering and absorption by such layered systems.

5.1 Cascading the cylindrical layers

The boundary value problem of the scattered cylindrical modes inside a set of concentric cylindrical layers leads to a system of linear equations. Utilizing a direct linear algebra method for obtaining the scattered cylindrical modes inside layers with losses or axially symmetric distribution of the dielectric function could be problematic due to typically large condition numbers of the system matrices. The algorithm that we use includes a normalization step, making it possible to improve poor conditioning. However, if the algorithm were used for getting analytical formulae the normalization would not be necessary.

We consider a concentric cylindrical device having $l-1$ layers, $r_i < r < r_{i+1}$, $i = \overline{1, l-1}$, with the "outer" ($r > r_s$) layer l filled with a host media, as shown in Fig. 2.

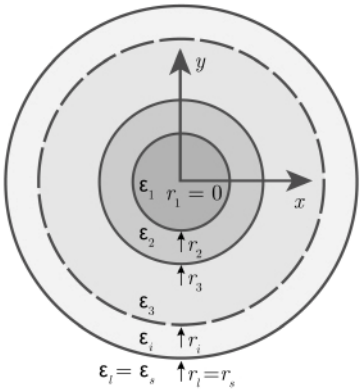

Fig. 2. Schematic geometry of the layered structure.

The general solution of the wave equation in i^{th} layer can be represented as a sum of angular harmonics, $f^i(r,\phi) = \sum_{m=-\infty}^{+\infty} f_m^i(r) \exp \imath m\phi$ where the radial part $f_m^i(r)$ consists of two partial solutions $R_m^i(r)$ and $T_m^i(r)$ with yet undefined coefficients. These coefficients can be obtained from appropriate $2l$ boundary conditions. All cylindrical modes are linearly independent, thus each of the boundary conditions can be separated into the individual equations for each m^{th} mode, similar to that shown in (14) presented in a more general form,

#126127 - $15.00 USD Received 30 Mar 2010; revised 19 Jun 2010; accepted 29 Jun 2010; published 23 Jul 2010

$$f^i_{(m)}(r) = \tau^i\, T^i(r)/T^i(r_i) + \rho^i\, R^i(r)/R^i(r_i),\ i = \overline{1,l},\ r_1 = r_2, \tag{32}$$

where for the simplicity of notation (and from now on in this section) we suppress the index m. To satisfy the condition (22) in the core layer we put $\rho^1 = 0$ and $T^1_{(m)}(r) = J_m(k_1 r)$.

Furthermore, the total field in the "outer" layer can be separated into the "incident" and "scattered" parts. The Sommerfeld radiation condition $R^l_{(m)}(r) = H^+_m(k_0 r)$ is imposed on the scattered field (cf. Eq. (23)), while for the incident wave $\tau^l_{(m)} = a_m J_m(\overline{r_s})$, with the values of the coefficients a_m taken from the expansion of the incident wave (25), (31).

To obtain the rest of $2l-2$ equations we use the standard boundary condition (20), (21) for TE polarization at each interface $r = r_{i+1}$,

$$\begin{bmatrix} 1 & 1 \\ L^{i,1}_T & L^{i,1}_R \end{bmatrix} \begin{bmatrix} \tau^{i+1} \\ \rho^{i+1} \end{bmatrix} = \begin{bmatrix} 1 & 1 \\ L^{i,0}_T & L^{i,0}_R \end{bmatrix} \mathrm{diag}(F^i_T, F^i_R) \begin{bmatrix} \tau^i \\ \rho^i \end{bmatrix}, \tag{33}$$

where $F^i_X = \dfrac{X^i(r_{i+1})}{X^i(r_i)}$, $L^{i,q}_X = \dfrac{X'^{i+q}}{X'^{i+q}}(r_{i+1})$, $X = R,T$, $q = 0,1$.

For the TM polarization the only change is that $L^{i,0}_X \to (\varepsilon_{i+1}/\varepsilon_i)(r_{i+1}) L^{i,0}_X$. Inverting the matrix at the left-hand-side of (33) and evaluating its determinant as $d^{i+1} = L^{i,1}_R - L^{i,1}_T = \dfrac{W[T^{i+1}, R^{i+1}]}{T^{i+1} R^{i+1}}(r_{i+1})$ we obtain

$$\begin{bmatrix} \tau^{i+1} \\ \rho^{i+1} \end{bmatrix} = w^i_m \begin{bmatrix} \tau^i \\ \rho^i \end{bmatrix},\ i = \overline{1,l-1}, \tag{34}$$

where

$$w^i_m = \frac{1}{d^{i+1}} \begin{bmatrix} F^i_T\left(L^{i,1}_R - L^{i,0}_T\right) & F^i_R\left(L^{i,1}_R - L^{i,0}_R\right) \\ -F^i_T\left(L^{i,1}_T - L^{i,0}_T\right) & -F^i_R\left(L^{i,1}_T - L^{i,0}_R\right) \end{bmatrix}, \tag{35}$$

and $W[T,R] = TR' - T'R$ is the Wronskian [12], which is taken for the partial solutions of the $i+1$ layer. In particular, for homogeneous layers we exploit the known value of the Wronskians for the Bessel functions [15],

$$\begin{aligned} &W[J_m, Y_m](x) = 2/\pi x; \\ &W[J_m, H^{\pm}_m](x) = \pm \imath 2/\pi x; \\ &W[H^+_m, H^-_m](x) = -\imath 4/\pi x. \end{aligned} \tag{36}$$

For a layer with the inverse-square radial dependence of the dielectric we have $T = r^{-\alpha + \imath\beta_m}$, $R = r^{-\alpha - \imath\beta_m}$ which yields $TRW^{-1}[T,R] = \imath r/(2\beta_m)$. This approach is also known as the 'cascading layers' method [16], since the solution in each layer (34) is then a composition of transfer matrices applied to the first layer $[\tau^{i+1}, \rho^{i+1}]^T = \left(\prod^1_{k=i} w^k\right)[\tau^1, \rho^1]^T$) [13].

The resulting system obtained after stating all 2*l* boundary conditions has the form:

#126127 - $15.00 USD Received 30 Mar 2010; revised 19 Jun 2010; accepted 29 Jun 2010; published 23 Jul 2010

$$\begin{cases} \rho^1 = 0 \\ \tau^{i+1} = w_{11}^i \tau^i + w_{12}^i \rho^i \\ \rho^{i+1} = w_{21}^i \tau^i + w_{22}^i \rho^i \\ \tau^l - \text{known, e.g., } a_{(m)}^{inc} J_m\left(\overline{r}_l\right) \end{cases}, \left(i \in \overline{1, l-1}\right) \tag{37}$$

The system (37) can be solved in two sweeps, similar to the standard Thomas algorithm [17]. In this approach, the auxiliary normalized coefficients $\overline{\tau}^i = \tau^{i+1} / \tau^i$, and $\overline{\rho}^i = \rho^i / \tau^i$, $\left(i \in \overline{1, l-1}\right)$ are calculated by forward sweep using the recurrence (38)

$$\begin{cases} \overline{\rho}^1 = 0 \\ \overline{\tau}^i = w_{11}^i + w_{12}^i \overline{\rho}^i \\ \overline{\rho}^{i+1} = \left(w_{21}^i + w_{22}^i \overline{\rho}^i\right) / \overline{\tau}^i \end{cases}, \quad \left(i \in \overline{1, l-1}\right) \tag{38}$$

followed by the backward sweep of the reflection and transmission coefficients (39), while using the initial condition at the external interface:

$$\begin{cases} \tau^i = \tau^{i+1} / \overline{\tau}^i \\ \rho^i = \overline{\rho}^i \tau^i \end{cases}, \left(i \in \overline{1, l-1}\right) \tag{39}$$

where τ^l is known and $\rho^l = \overline{\rho}^l \tau^l$.

The above algorithm includes the normalization of the partial solution in each layer by its value on the inner interface (the field in the core layer is an exception and is normalized by its value on the outer interface $r = r_2$, the latter is achieved by substitution $r_1 = r_2$ in Eq. (32)). The normalization significantly improves the accuracy of the mathematical operations, performed numerically with a limitation of floating-point representations and arithmetic. Finally, the procedure yields the m^{th} mode of the field by using (32); the solution to the entire problem in the i^{th} layer is given as a sum of the angular momentum modes, $f^i(r, \phi) = \sum_{m=-\infty}^{\infty} f_m^i(r) e^{\imath m \phi}$.

5.2 Scattering and absorption efficiencies

For any optical system, scattering and absorption efficiencies have the physical meaning of the relative size of the equivalent "black body" target which results in the same amount of scattered and absorbed power [18].

First, we recapitulate that the *total field* $\mathbf{E} = \hat{\mathbf{z}} f$ (TE) or $\mathbf{H} = \hat{\mathbf{z}} f$ (TM) outside the device at the external boundary of the shell, $r = r_s$ is defined as ($e^{-\imath \omega t}$ is omitted)

$$f = \sum_{m=-\infty}^{+\infty} f_m(\overline{r}_s) \exp \imath m \phi. \tag{40}$$

Then, we assume that the m^{th} mode of the total field is given by,

$$f_m = H_m^- + c_m^+ H_m^+, \tag{41}$$

or

$$f_m = 2J_m + \left(c_m^+ - 1\right) H_m^+, \tag{42}$$

so that the total field (40) is decomposed into a plane wave illumination source

#126127 - $15.00 USD Received 30 Mar 2010; revised 19 Jun 2010; accepted 29 Jun 2010; published 23 Jul 2010

$$f_{inc} = 2\sum\nolimits_m J_m = 2e^{\imath ky}, \tag{43}$$

and the scattered field

$$f_{sca} = \sum\nolimits_{m=-\infty}^{\infty} (c_m^+ - 1) H_m^+ \exp \imath m\varphi, \tag{44}$$

where coefficients c_m^+ are determined from the boundary value problem. In (41)-(44) and further on we use abbreviations J_m, $H_m^{\pm}$ for $J_m(\overline{r}_s)$, $H_m^{\pm}(\overline{r}_s)$.

Equations (40)-(43) are used for the time-averaged Poynting vector $\mathbf{S}^{abs} = \frac{1}{2}\mathrm{Re}\left(\mathbf{E}\times\mathbf{H}^*\right)$, and its normalized radial component $S_r^{abs} = \hat{\mathbf{r}}\cdot\mathbf{S}/W$, where W is the total power transmitted by the incident wave through $2r_s$ –wide strip per its unit length:

$$S_r^{abs} = \tfrac{1}{8\overline{r}_s}\hat{\mathbf{r}}\cdot\mathrm{Re}\left[\hat{\mathbf{z}}f\times\left(\imath\nabla f\times\hat{\mathbf{z}}\right)^*\right] = \tfrac{1}{8\overline{r}_s}\mathrm{Im}\left(f^*\frac{\partial f}{\partial\overline{r}_s}\right), \tag{45}$$

and since the absorption efficiency per unit length is taken as a normalized flux of power flowing into the device, $Q^{abs} = -\int_0^{2\pi} S_r^{abs} r_s d\phi$, $f_m' = df_m / d\overline{r}_s$ we arrive at

$$Q^{abs} = -\frac{\pi}{4}\sum_{m=-\infty}^{\infty}\mathrm{Im}\left(f_m^* f_m'\right). \tag{46}$$

After applying (41) to (46), we note that $\mathrm{Im}\left(f_m^* f_m'\right)$ includes a vanishing sum of a complex number with its conjugate, $\mathrm{Im}\left[\left(c_m^+ H_m^+ H_m^{+\prime}\right)^* + c_m^+ H_m^+ H_m^{+\prime}\right] = 0$, and another term, $\mathrm{Im}\left[\left(H_m^- H_m^{+\prime}\right)^* + \left|c_m^+\right|^2 H_m^- H_m^{+\prime}\right] = -\left(1-\left|c_m^+\right|^2\right)\mathrm{Im}\left(H_m^- H_m^{+\prime}\right)$, so that

$$Q^{abs} = \frac{1}{2\overline{r}_s}\sum_{m=-\infty}^{\infty}\left(1-\left|c_m^+\right|^2\right); \tag{47}$$

which is obtained by substituting $\mathrm{Im}\left(H_m^- H_m^{+\prime}\right) = W\left(J_m, Y_m\right)$ with $2/\left(\pi\overline{r}_s\right)$ (cf. Eq. (36)).

Similarly the scattering efficiency per unit length is calculated by taking the flux of normalized power of the scattered field (44) moving away from the device, $Q^{sca} = \int_0^{2\pi} S_r^{sca} r_s d\phi$, where likewise (45), $S_r^{sca} = \frac{1}{8r_s}\mathrm{Im}\left(f_{sca}^*\frac{\partial f_{sca}}{\partial\overline{r}_s}\right)$; and we obtain

$$Q^{sca} = \frac{1}{2\overline{r}_s}\sum_{m=-\infty}^{\infty}\left|1-c_m^+\right|^2. \tag{48}$$

Note that if the solution of the same scattering problem is given for an arbitrary source of illumination as $f_m = \tilde{c}_m^- H_m^- + \tilde{c}_m^+ H_m^+$, then due to the linearity of the problem the coefficients relate to those from (41) as $c_m^+ = \tilde{c}_m^+ / \tilde{c}_m^-$. In particular this gives immediate expressions for the absorption and scattering efficiencies, if the total field is given as $f_m = a_m J_m + b_m H_m^+$ for which $\tilde{c}_m^- = \frac{1}{2}a_m$, $\tilde{c}_m^+ = b_m + \frac{1}{2}a_m$; then substitution $c_m^+ = \tilde{c}_m^+ / \tilde{c}_m^- = 1 + 2a_m^{-1}b_m$ and the use of $a_m = \imath^m$ gives

#126127 - $15.00 USD Received 30 Mar 2010; revised 19 Jun 2010; accepted 29 Jun 2010; published 23 Jul 2010

$$Q^{abs} = -\frac{2}{\bar{r}_s}\sum_{m=-\infty}^{\infty}\left(\mathrm{Re}\left[\iota^{-m}b_m\right]+\left|b_m\right|^2\right), \tag{49}$$

$$Q^{sca} = \frac{2}{\bar{r}_s}\sum_{m=-\infty}^{\infty}\left|b_m\right|^2. \tag{50}$$

5.3 The ideal electromagnetic black hole

We consider the ideal "fundamental" ($p = 2$) electromagnetic black hole, see (1), (2), (3). It is a three layered system with a gradient-index shell and absorbing core, for which the formalism of Section 5.1 can be applied to calculate the exact full-wave solution. Fig. 3 shows an example simulation of an ideal black hole with $\varepsilon_s = 2.1$, $r_s = 20\,\mu\mathrm{m}$, and $r_c = 8.367\mu\mathrm{m}$. The device is illuminated with a Gaussian beam (free-space wavelength $\lambda = 1.5\mu\mathrm{m}$ and full width $w = 2\lambda$), which is focused at fixed x_0, and different y_0 (where $x_0 = 0$, and $y_0/r_s = 1.5,\ 1,\ 0.75$, and 0).

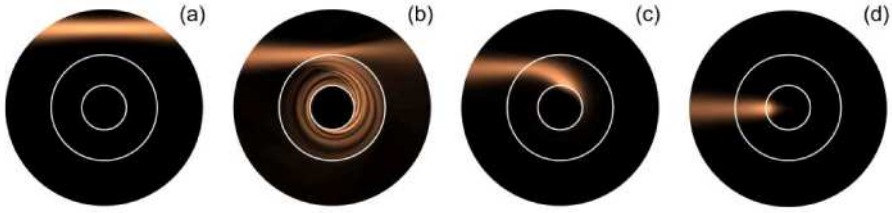

Fig. 3. (Media 1) Ideal black hole with $\varepsilon_s = 2.1$, $\varepsilon_c = 12$, $\gamma_c = 0.7$, $r_s = 20$ µm, and $r_c = r_s(\varepsilon_s/\varepsilon_c)^{1/2} = 8.367$ µm. The Gaussian beam with free-space wavelength $\lambda = 1.5$µm and full width $w = 2\lambda$ is focused at $x_0 = 0$, and (a) $y_0 = 1.5r_s$; (b) $y_0 = r_s$; (c) $y_0 = 0.75r_s$, and (d) $y_0 = 0$. Range of modes used in series from (a) to (d): [-50;50], [-140;-40], [-170;-70], [-230;-130]

Furthermore the approach is also used to determine the final form of the absorption efficiency. For this we use Eqs. (47), (48) and derive the scattering coefficients. We write the total field outside the device as $f_m^3(\bar{r}) = H_m^-(\bar{r}) + c_m^+ H_m^+(\bar{r}) = \tau_m^3 H_m^-(\bar{r})/H_m^- + \rho_m^3 H_m^+(\bar{r})/H_m^+$, where $\tau_m^3 = H_m^-$, $\rho_m^3 = c_m^+ H_m^+$. Then the exact formula for the scattering coefficients is given as

$$c_m^+ = \frac{\rho_m^3}{H_m^+} = \left(H_m^-/H_m^+\right)\left[\left(w_{21}^2 w_{11}^1 + w_{22}^2 w_{21}^1\right)/\left(w_{11}^2 w_{11}^1 + w_{12}^2 w_{21}^1\right)\right]_m. \tag{51}$$

The coefficients w_{ij}^k are readily available from (35), then writing the explicit expressions for the matrix elements to (51) we obtain:

$$c_m^+ = -\frac{H_m'^- + \eta_m H_m^-}{H_m'^+ + \eta_m H_m^+}, \tag{52}$$

where

$$\eta_m = \frac{\beta_m}{\bar{r}_s}\left[\frac{\alpha}{\beta_m} - \iota\frac{1-X}{1+X}\right],\quad X = \frac{1+\iota Y}{1-\iota Y}\left(\frac{r_c}{r_s}\right)^{\iota 2\beta_m},\quad Y = \frac{\alpha}{\beta_m} + A\frac{\bar{r}_c J_m'(\bar{r}_c)}{\beta_m J_m(\bar{r}_c)}.$$

The coefficients $-\alpha \pm \iota\beta_m$ are the characteristic roots of the Euler equation (cf. Eq. (19)), and factor A is obtained from the boundary conditions,

#126127 - $15.00 USD Received 30 Mar 2010; revised 19 Jun 2010; accepted 29 Jun 2010; published 23 Jul 2010

$$\begin{array}{lccc} & \alpha & \beta_m & A \\ \text{TE} & 0 & \sqrt{\bar{r}_s^2 - m^2} & 1 \\ \text{TM} & 1 & \sqrt{\bar{r}_s^2 - m^2 - 1} & \varepsilon_c / \left(\varepsilon_c + \imath \gamma_c \right) \end{array} \tag{53}$$

For reshaping η_m we use the identity $-\imath(1-X)/(1+X) = \tan\left(\frac{\imath}{2}\ln X\right)$. Similarly in the expression for X, we use the identity $(1+\imath Y)/(1-\imath Y) = \exp\left(\imath 2 \tan^{-1} Y\right)$ so that coefficients η_m can be written for both polarizations as

$$\eta_m = \frac{\beta_m}{\bar{r}_s}\left[\frac{\alpha}{\beta_m} - \tan\left(\beta_m \ln\frac{r_c}{r_s} + \tan^{-1}\left[\frac{\alpha}{\beta_m} + A\frac{\bar{r}_c J_m'(\bar{r}_c)}{\beta_m J_m(\bar{r}_c)}\right]\right)\right]. \tag{54}$$

5.4 The lamellar electromagnetic black hole

The formalism of a layered system for example can be used to study a non-ideal lamellar "black hole" optical concentrator and absorber, which approximates an ideal device ($\varepsilon_s = 2.1$, $r_s = 20\,\mu\text{m}$, and $r_c = 8.367\mu\text{m}$) with a different number of homogeneous layers, *l.* The device is illuminated by a plane wave with free-space wavelength $\lambda = 1.5\mu\text{m}$; for *l* equal to 3, 5, 9, and 17. Scattering and absorption efficiencies are given in (49)-(50), the latter, Q^{abs}, yields 72%, 84%, 90%, and 94% respectively. Fig. 4(e) depicts the field map of the ideal black hole with smooth gradient, where 99% absorption efficiency is achieved.

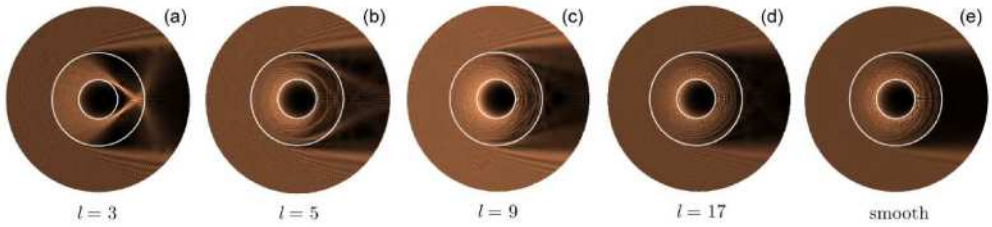

Fig. 4. Simulated field maps for a lamellar "black hole" optical concentrator and absorber (ε_s = 2.1, r_s = 20 μm, and r_c = 8.367 μm) vs. the total number of layers, *l.* The device is illuminated by a plane wave with free-space wavelength λ = 1.5μm. (a) *l* = 3, and 72% absorption efficiency, (b) *l* = 5, and 84% absorption efficiency, (c) *l* = 9, and 90% absorption efficiency, (d) *l* = 17, and 94% absorption efficiency. Panel (e) depicts the reference case of the ideal black hole with smooth gradient, and 99% absorption efficiency.

6. Semiclassical description

The primary objective of the present section is the derivation of the semiclassical expansion ($\bar{r}_s \gg 1$) of the scattering and absorption cross sections of the "fundamental" (*p* = 2) electromagnetic black hole, introduced in Section 2.

Intuitively, from the ray dynamics of Section 2, we expect the absorption cross section to be close to the "geometrical" limit, so that $Q^{abs} \to 1$. The ray-optical treatment of Section 5 however gives no quantitative measure of how closely this limit is actually approached in a practical device. On the other hand, the exact description of Section 5, while giving a precise quantitative account, provides no compact lucid description of the system behavior. In contrast to this behavior, the semiclassical approach, mathematically corresponding to taking the formal limit $\bar{r}_s \gg 1$ of the exact solution, combines the clear physical picture of the actual dynamics in terms of the underlying ray trajectories, with the quantitative description of the interference and diffraction in the system.

#126127 - $15.00 USD Received 30 Mar 2010; revised 19 Jun 2010; accepted 29 Jun 2010; published 23 Jul 2010

The semiclassical approximation for the reflection coefficients and the absorption cross-section can be obtained by taking the limit $\overline{r}_s \gg 1$ in (52) and (54). Mathematically, this corresponds to the famous Debye expansion [12] of the Bessel functions

$$H_m^{\pm}(x) = \sqrt{\frac{2}{\pi\sqrt{x^2-m^2}}}\left[1+O\left(\frac{1}{\sqrt{x^2-m^2}}\right)\right]\exp\left[\pm\imath\sigma_m(x)\right], \tag{55}$$

where the "phase" $\sigma_m(x) = \sqrt{x^2-m^2} - m\cos^{-1}(m/x) - \pi/4$.

Physically, the angular momenta summation in absorption efficiency (47) can be separated into two parts – the sum over $|m| < \overline{r}_s$ and the sum over $|m| > \overline{r}_s$. As the dimensionless angular momentum m has physical meaning of the product of the (fixed) wavenumber and the impact parameter – see Fig. 2 – the sum over $|m| < \overline{r}_s$ corresponds to the rays that actually hit the target and as a result experience strong scattering. On the other hand, the sum for $|m| > \overline{r}_s$ takes into account the rays that miss the object. In the geometrical-optics limit, those rays experience no scattering and thus do not contribute to the cross-section. Beyond ray optics, the waves with $|m| > \overline{r}_s$, do experience some amount of scattering normally associated with diffraction, however in the limit $\overline{r}_s \gg 1$ the resulting contribution is exponentially small. Therefore, in the semiclassical limit $\overline{r}_s \gg 1$ the sum over large angular momenta ($|m| > \overline{r}_s$) can be neglected, and we obtain

$$Q^{abs} \approx \tfrac{1}{2\overline{r}_s}\sum_{|m|\le\overline{r}_s}\left(1-\left|c_m^+\right|^2\right). \tag{56}$$

Furthermore, for $\overline{r}_s \gg 1$ the relative change in $\left|c_m^+\right|$, when one goes from m to $m+1$, is reasonably small – leading to the relative error $\sim 1/\overline{r}_s$ – and thus the summation in Eq. (56) can be approximated by the integral

$$Q^{abs} \approx \tfrac{1}{2\overline{r}_s}\int_{-\overline{r}_s}^{\overline{r}_s} dm\left(1-\left|c_m^+\right|^2\right). \tag{57}$$

Note that in this approximation the values of the parameter β_m that are different for the TE and TM polarization (cf. Eq. (53)), should be considered equal, i.e. $\sqrt{\overline{r}_s^2-m^2-1} \approx \sqrt{\overline{r}_s^2-m^2}$, then, applying Debye approximation to (52) and using identity $(1+\imath Y)/(1-\imath Y) = \exp\left(\imath 2\tan^{-1}Y\right)$ we obtain,

$$c_m^+ = \exp\left\{\imath 2\left[\tan^{-1}\left(\frac{\overline{r}_s}{\beta_m}\eta_m - \frac{1}{2}\frac{\overline{r}_s^2}{\beta_m^3}\right) - \sigma_m\left(\overline{r}_s\right)\right]\right\}. \tag{58}$$

Furthermore, for $\overline{r}_s \gg 1$ the term $-\frac{1}{2}\overline{r}_s^2/\beta_m^3$ can be neglected, in addition, from (54) we have

$$\frac{\overline{r}_s}{\beta_m}\eta_m = \frac{\alpha}{\beta_m} - \tan\left(\beta_m \ln\frac{r_c}{r_s} + \tan^{-1}\left[\frac{\alpha}{\beta_m} + A\frac{\overline{r}_c J_m'(\overline{r}_c)}{\beta_m J_m(\overline{r}_c)}\right]\right), \tag{59}$$

#126127 - $15.00 USD Received 30 Mar 2010; revised 19 Jun 2010; accepted 29 Jun 2010; published 23 Jul 2010

and since the fraction α/β_m is very small for the TM polarization and is exactly equal to zero for TE polarization, using the Debye expansion for Bessel function in the limit $\bar{r}_s \gg 1$ and low losses in (59) we obtain,

$$\tan^{-1}\left(\frac{\bar{r}_s}{\beta_m}\eta_m\right) = -\beta_m \ln\frac{r_c}{r_s} - \tan^{-1}\left[A\frac{\bar{r}_c J'_m(\bar{r}_c)}{\beta_m J_m(\bar{r}_c)}\right]. \tag{60}$$

Using a similar approximation for $J_m(\bar{r}_c) \approx \sqrt{\frac{1}{2\pi\sqrt{\bar{r}_c^2 - m^2}}}\cos\left[\sigma_m(\bar{r}_c)\right]$ in (60) we write,

$$\begin{aligned}\tan^{-1}\left(\frac{\bar{r}_s}{\beta_m}\eta_m\right) &= -\beta_m \ln\frac{r_c}{r_s} \\ -\tan^{-1}&\left[-A\left(\frac{1}{2}\frac{\bar{r}_c^2}{\beta_m(\bar{r}_c^2 - m^2)} + \frac{\sqrt{\bar{r}_c^2 - m^2}}{\beta_m}\tan\left[\sigma_m(\bar{r}_c)\right]\right)\right],\end{aligned} \tag{61}$$

where phase factor $\sigma_m(\bar{r}_c)$ is already defined in (55), and $\bar{r}_c = k_c r_c$.

Then, dropping the small term $\frac{1}{2}\bar{r}_c^2 \Big/ \left[\beta_m(\bar{r}_c^2 - m^2)\right]$ and taking $A\sqrt{\bar{r}_c^2 - m^2}\Big/\beta_m \approx 1$ (due to small losses) in (61), we are back to (58) and obtain,

$$c_m^+ = \exp\left\{-\imath 2\left[\beta_m \ln\frac{r_c}{r_s} - \sigma_m(\bar{r}_c) + \sigma_m(\bar{r}_s)\right]\right\}, \tag{62}$$

with the magnitude of (62) being

$$\left|c_m^+\right| = \exp\left\{-\frac{\gamma_c}{\varepsilon_c}\sqrt{\bar{r}_s^2 - m^2}\right\}, \tag{63}$$

where we used, $\sigma_m(\bar{r}_c) - \sigma_m(\bar{r}_s) \approx \frac{\imath}{2}\frac{\gamma_c}{\varepsilon_c}\sqrt{\bar{r}_s^2 - m^2}$.

For the absorption efficiency (57) after substitution (63) we then obtain,

$$Q^{abs} \approx \frac{1}{2\bar{r}_s}\int_{-\bar{r}_s}^{\bar{r}_s}\left(1 - \exp\left(-2\frac{\gamma_c}{\varepsilon_c}\sqrt{\bar{r}_s^2 - m^2}\right)\right)dm, \tag{64}$$

and after variable substitution (64) can be written as a standard integral

$$Q^{abs} = 1 - F\left(2\bar{r}_s\frac{\gamma_c}{\varepsilon_c}\right) = \frac{\pi}{2}\left[I_1\left(2\bar{r}_s\frac{\gamma_c}{\varepsilon_c}\right) - L_1\left(2\bar{r}_s\frac{\gamma_c}{\varepsilon_c}\right)\right], \tag{65}$$

where I_1 and L_1 are the modified Bessel and Struve functions of the first order, and

#126127 - $15.00 USD Received 30 Mar 2010; revised 19 Jun 2010; accepted 29 Jun 2010; published 23 Jul 2010

$$F(x)=\int_0^{\pi/2}\cos\theta\exp(-x\cos\theta)\,d\theta$$

$$=1-\frac{\pi}{2}\left[I_1(x)-L_1(x)\right]=\begin{cases}1-\frac{1}{2}x+O\left(x^2\right), & x\ll 1\\ \dfrac{1}{x^2}+O\left(\dfrac{1}{x^4}\right), & x\gg 1\end{cases} \tag{66}$$

Equations (65) and (66) finalize the derivation of the semiclassical expansion ($\overline{r}_s \gg 1$) of the scattering and absorption cross sections of the "fundamental" ($p=2$) electromagnetic black hole, which is the specific aim of this Section. As expected, for both polarizations in the absence of losses we find zero absorption cross-section. However, even for moderate losses $\gamma_c/\varepsilon_c \sim 1/\overline{r}_s$ the absorption efficiency is close to one. Thus, as predicted by the semiclassical theory, the device does indeed absorb nearly all the incident light from every direction.

To further illustrate our results we first qualitatively portray the decay of performance as we move away from the semiclassical limit. Fig. 5 shows field patterns of the black hole device ($\varepsilon_s = 2.1$, $r_s = 20\mu$m, r_s = 20 μm, and $r_c = 8.367\mu$m) illuminated by a TE-polarized plane wave for a free-space wavelength changing from 1.5 to 6.0 μm, where increasing scattering is observed with increase of wavelength. Then, we perform a quantitative comparison of the absorption efficiency, Q^{abs}, versus the ratio λ/r_s.

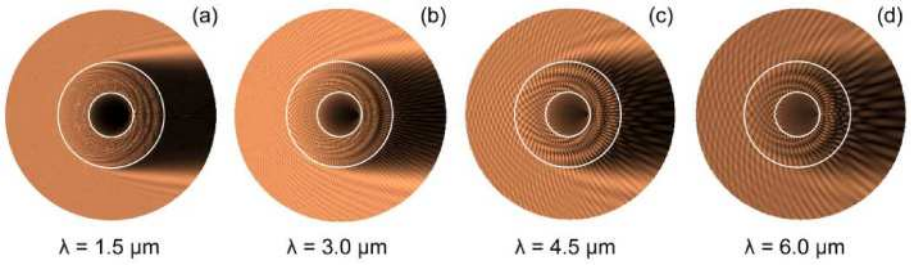

Fig. 5. Field patterns of the black hole device (ε_s = 2.1, r_s = 20 μm, and r_c = 8.367 μm) illuminated by a TE-polarized plane wave with a free-space wavelength of (a) 1.5 μm, (b) 3.0 μm, (c) 4.5 μm, and (d) 6.0 μm.

The efficiencies, shown in Fig. 6a, are separately calculated for the TE- and TM-polarized plane wave using the exact method of Section 5, and the semiclassical result of Section 6, which is valid for both polarizations. Figures 6a also indicates good quality of the semiclassical approximation of the absorption cross-section even far beyond the semiclassical limit. Figure 6b depicts a more detailed plot for λ/r_s changing from 0.075 to 0.15.

#126127 - $15.00 USD Received 30 Mar 2010; revised 19 Jun 2010; accepted 29 Jun 2010; published 23 Jul 2010

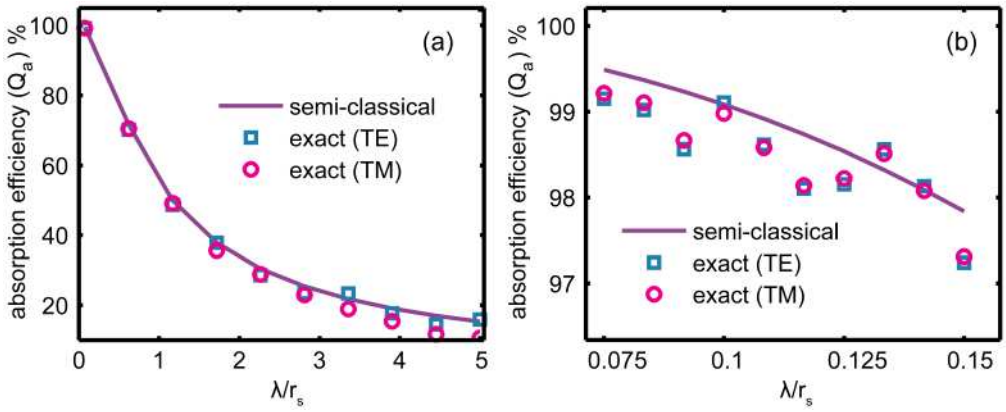

Fig. 6. (a) Absorption efficiency Q_a vs. the ratio λ/r_s obtained for the TE- and TM-polarized plane wave; (b) a more detailed plot for the ratios from 0.075 to 0.15.

7. Summary

In summary, we have developed a theoretical description of wave propagation in cylindrically-symmetric gradient-index systems, and applied this approach to light "trapping" in the recently proposed electromagnetic black hole concentrator and absorber.

In particular we have demonstrated that an approximate lamellar black-hole with a relatively limited number of homogeneous layers, while giving the desired ray-optical performance, can provide absorption efficiencies comparable with those of ideal devices with smooth gradients in index. It is forecasted that the use of non-uniform layers could further improve the performance of the lamellar device with a given number of homogeneous layers. The numerical validation of the mathematical apparatus for designing the black-hole devices opens the path for the development of test beds that could further advance the application of this light-trapping technique into a viable commercial option.

Acknowledgments

This work was partially supported by ARO MURI 56154-PH-MUR, 50342-PH-MUR, and also through IIP SB RAS No 113, and RFFS No 09-01-00352-a.

#126127 - $15.00 USD Received 30 Mar 2010; revised 19 Jun 2010; accepted 29 Jun 2010; published 23 Jul 2010